Using Carrier Frequency Current Injection for the Estimation of Flux, Position, and Velocity in AC Drives

L.A.S. Ribeiro[1], M.W. Degner[2], F. Briz[3], and R.D. Lorenz[4]

[1] Dept. of Elect. Engineering
Centro Federal de Educação Tecnológica do Maranhão
Av. Getúlio Vargas, 04 São Luís, Ma 65025-001, Brazil
Tel.: +55-98-218-9080 Fax: +55-98-218-9019
Email: lantonio@cefet-ma.br

[2] Ford Research Laboratory
Ford Motor Company
Dearborn, MI 48121, USA
Tel: 313-322-6499 Fax: 313-323-8239
Email: mdegner@ford.com

[3] Dept. of Elect., Comp. & Systems Engineering
University of Oviedo
Gijon 33208, Spain
Tel: 34-985-14-4632 Fax: 34-985-18-2068
Email: fernando@isa.uniovi.es

[4] Dept. of Mech. Eng. and Dept. of Elec. & Comp. Eng.
University of Wisconsin-Madison
Madison, WI 53706, USA
Tel: 608-262-5343 Fax: 608-265-2316
Email: lorenz@engr.wisc.edu

***Abstract* – The focus of this paper is on an analysis of position, velocity, and flux estimation in ac machines based on the injection of a carrier signal in addition to the fundamental excitation. Specifically the paper addresses two problems of carrier signal current injection: 1) the regulation of high frequency currents with current regulators of limited bandwidth (regulation of the carrier signals with zero steady-state error is necessary to avoid loss of spatial information), and 2) the extraction of the spatial information contained in the induced voltages.**

I. Introduction

The use of carrier signal injection superimposed on the fundamental component to track spatial saliency images has established itself in recent years as a viable means of eliminating position sensors in AC drives for applications requiring true, sustained, zero speed, zero frequency torque (and often also motion) control [1-8].

Voltage and current have both been used for such carrier signal injection, the tradeoffs involved in using one over the other has been evaluated previously in [9]. Carrier signal voltage injection has an advantage over carrier signal current injection with a traditional voltage source inverter since it is relatively easy to produce the desired excitation. Carrier signal current injection has the potential advantage over carrier signal voltage injection of providing a fairly large voltage signal, which contains the desired spatial information, relative to the amount of current injected due to the increase in magnitude of the impedance (inductive reactance) with frequency.

Current injection also has numerous potential difficulties. First, the relatively low frequency carrier signal used with some of the proposed current injection techniques [5, 6] diminishes the advantage provided by the impedance magnitude frequency gain, requiring a relatively larger magnitude of injected (current) signal. Second, when a lower frequency carrier signal current is used, the higher amplitude carrier signal produces increased torque ripple. Third, the rather minimal spectral separation makes isolating the carrier frequency content from the fundamental excitation more difficult while simultaneously reducing the estimation bandwidth. Fourth, carrier signal current injection requires a current regulator of sufficient bandwidth to properly regulate both the fundamental and the carrier signal currents. Such performance is often beyond that of the standard synchronous frame PI current regulator.

This paper first develops methods that allow the injection of a higher frequency carrier signal current than used previously [5, 6]. The injection of a higher frequency carrier signal current substantially mitigates the problems associated with using a low carrier signal frequency. The paper then focuses on the extraction of the spatial information contained in the induced voltages. Finally the paper presents some experimental results of the proposed technique.

II. Flux, Position, and Velocity Estimation Utilizing Spatial Saliencies

In this paper it will be assumed that the machine contains a single sinusoidal spatial saliency. The spatial saliency can be a result of a deterministic, rotor spatial modulation [1-8] or saturation due to the rotor, stator, or air-gap flux [2,9].

Injection of a balanced, poly-phase, carrier signal current vector (1) into a salient machine will impress a carrier signal voltage, which contains information relating to the spatial position of the saliency.

$$i_{s,qds_c} = I_{sc}\, e^{j\omega_c t} \tag{1}$$

Such carrier signal current excitation can be superimposed on the fundamental excitation using a pulsewidth modulated voltage source inverter (PWM-VSI) as shown in Fig. 1.

If the frequency of the carrier signal excitation, ω_c, is chosen so that it is substantially faster than the stator dynamics (stator transient time constant), modeling the machine using only the stator transient inductance is a good approximation [8]. In this case, the high frequency machine model can be written as (3).

$$v_{s,qds_c} \cong j\omega_c\, L_{s,\sigma s}\, i_{s,qds_c} \tag{3}$$

For a machine with a single sinusoidally distributed saliency, the stator transient inductance, in the stationary frame, can be represented by the following matrix, (4).

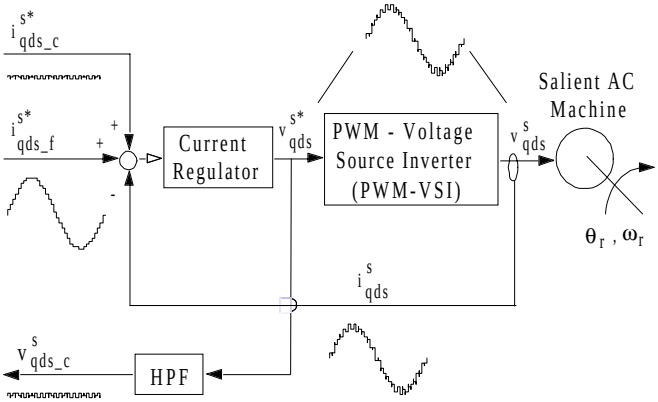

Figure 1: Injection of Carrier Signal Current Excitation using a PWM-VSI

$L_{s,\sigma s}$ =

Erro! (4)

where $\Sigma L_{\sigma s}$ = **Erro!**$(L_{\sigma qs} + L_{\sigma ds})$ is the average stator transient inductance,

$\Delta L_{\sigma s}$ = **Erro!**$(L_{\sigma qs} - L_{\sigma ds})$ is the differential stator transient inductance,

$L_{\sigma qs}$, $L_{\sigma ds}$ are the q and d stator transient inductances

θ_e is the position of the saliency in electrical degrees, and

h is the harmonic number of the saliency.

The interaction between the carrier signal current vector and the machine saliency will produce a carrier signal voltage (5), which contains information directly relating to the position of the saliency.

$$v_{s,qds_c} = v_{s,qds_cp} + v_{s,qds_cn} \quad (5)$$

where

$v_{s,qds_cp} = jV_{c_p}\, e^{j\omega_c t}$ is the positive sequence component,

$v_{s,qds_cn} = jV_{c_n}\, e^{j(h\theta_e - \omega_c t)}$ is the negative sequence component,

$V_{c_p} = \omega_c\, \Sigma L_{\sigma s} I_{sc}$, and $V_{c_n} = \omega_c\, \Delta L_{\sigma s} I_{sc.}$

The induced carrier signal voltage consists of both positive and negative sequence components in the stationary reference frame relative to the carrier signal excitation. The positive sequence component contains no spatial information and is proportional to the average stator transient inductance. The negative sequence component contains spatial information in its phase and is proportional to the differential stator transient inductance. The relative directions that the carrier signal voltage vectors rotate are shown in Fig. 2.

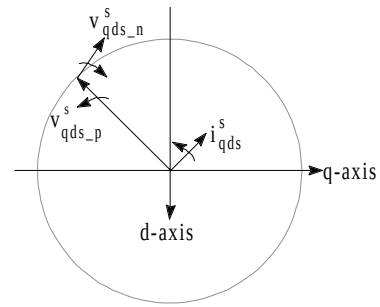

Figure 2: Induced Carrier Signal Voltages Produced by a Rotating Carrier Signal Current Vector Excitation in a Salient Machine

Fig. 3a shows the carrier signal voltage vectors drawn for several carrier signal injection angles, θ_c. From this plot it can be seen that the positive sequence component of the carrier signal voltage vector traces out a circular pattern and that the overall carrier signal voltage vector traces out an elliptical pattern. The elliptical pattern is a result of the two vectors that make up the overall carrier signal voltage vector rotating in opposite directions. The orientation of this ellipse relative to the coordinate system, i.e. the angle from the major axis of the ellipse to the q-axis, is a function of the saliency position. For this figure the position of the saliency with respect to the q-axis is $\theta_e = 0^o$. Fig. 3b shows the path traced out by the carrier signal current vector for another saliency position ($\theta_e = 60^o$). By comparing Figs. 3a and 3b, the rotation of the ellipse as the saliency rotates can be seen.

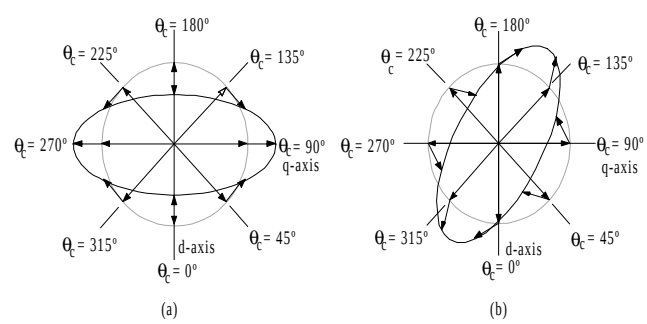

Figure 3: Elliptical Pattern Traced Out by the Carrier Signal Voltage Vectors in a Salient Machine: a) $\theta_e = 0^0$; b) $\theta_e = 60^0$

Because only the negative sequence component contains saliency position information it is desirable to filter off the positive sequence component. This can be done nearly ideally using a simple high-pass filter implemented in a reference frame synchronous with the positive sequence carrier signal [7, 8]. After filtering off the fundamental and carrier signal positive sequence components of the stator voltage, a tracking observer can be used to extract the spatial information contained in the phase of the negative sequence component of the carrier signal voltage.

Fig. 4 shows the block diagram of the tracking observer used to track rotor position when there is a rotor-position-dependent saliency present in the machine (note $\theta_e = \theta_r$ for a 2 pole machine). The tracking observer consists of 4 parts: 1) the cross-product between the estimated and actual negative sequence carrier signal voltage vectors, which generates an error signal proportional to the sine of

the phase error between the actual and the estimated vectors; 2) the controller, that forces the error to zero; 3) the mechanical system model, that models the dynamics of the actual system and provides an estimate of the rotor velocity in addition to the rotor position, this model includes a torque feedforward path which gives to the observer zero lag properties; and 4) a saliency model used to produce the estimated negative sequence carrier signal voltage vector.

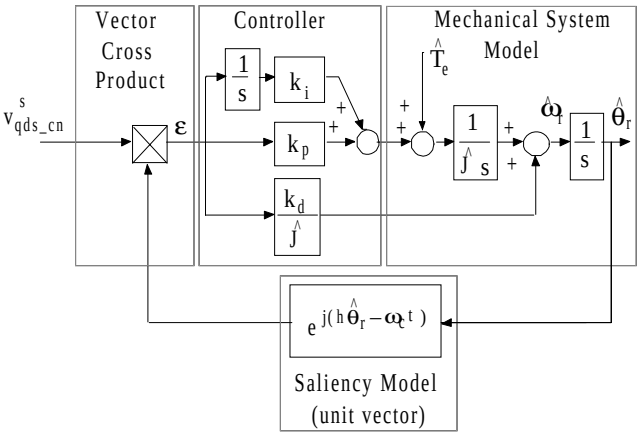

Figure 4: Zero-Lag Tracking Observer Used to Estimate Rotor Position in a Machine with a Single Rotor Position Dependent Saliency

The assumption used in this section of ideal current regulation would not be true in general when using a simple synchronous frame PI current regulator, especially if the signal being regulated is a high frequency signal and the current regulator has limited bandwidth. In the next section the problems associated with injecting a carrier current vector will be addressed.

III. Effect of Non-Ideal Current Regulation

Fig. 5 shows the voltage and current spectrums (ignoring inverter harmonics) for an idealized case of carrier signal current injection.

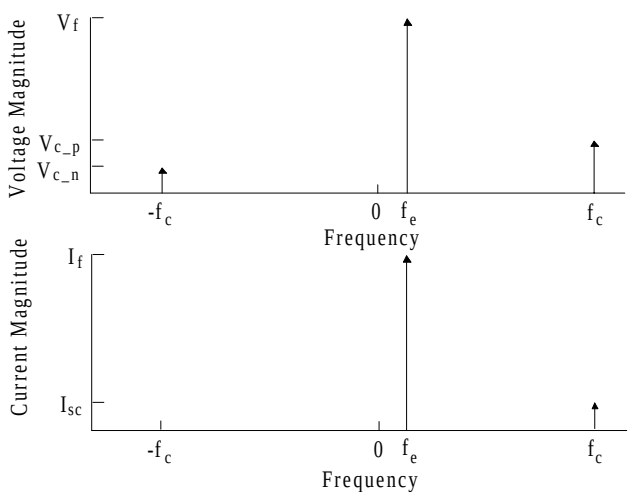

Figure 5: Idealized Voltage and Current Spectrums for Current Injection

The current spectrum has only the fundamental (I_f) and positive sequence carrier (I_{sc}) components. All of the desired saliency position information will be present in the negative sequence carrier signal component of the voltage, whose spectrum contains the fundamental (V_f), positive sequence carrier signal (V_{c_p}), and the negative sequence carrier signal (V_{c_n}) components. This idealized case is possible only if the current regulator is capable of regulating both the carrier and fundamental currents with zero steady-state error.

Because typical machine drives use voltage source inverters, the injection of a carrier signal current requires a current regulator that is capable of regulating a small, high frequency signal precisely. If the current regulator fails in regulating the carrier signal current with almost zero error, the carrier signal current itself will have both positive and negative sequence components, causing a loss of spatial information in the negative sequence carrier signal voltage.

This result can be seen in Fig. 6, which shows the measured voltage and current spectrums for the case of current injection. The test system had a PI current regulator with a bandwidth of 500 Hz and an induction machine with a deterministic 10% rotor slotting saliency, i.e. the difference between the q and d axis terminal impedance at 910 kHz is 10%. The carrier frequency for this case was f_c = 910 Hz. The carrier signal current command was 5.52 A, and the measured carrier current was 2.0 A. This difference between the commanded and measured carrier currents is due to the low bandwidth of the current regulator. The expected theoretical values for the positive and negative sequence carrier voltage signals are 1.2 V and 0.12 V, respectively. The measured positive and negative sequence carrier voltage signals are 1.15 V and 0.06 V, respectively.

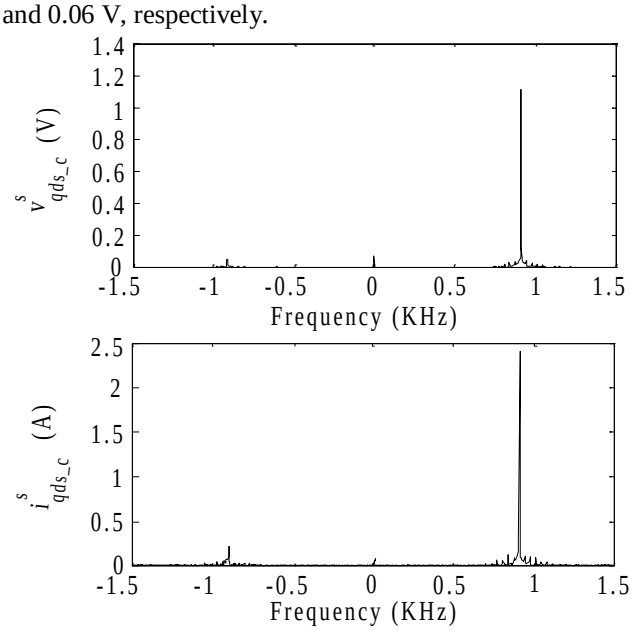

Figure 6: Measured Complex Voltage and Current Spectrums for Current Injection: ω_r=5 rpm, f_c = 910 Hz,

The measured negative sequence carrier signal voltage is only 50% of the theoretical value for this case. The imperfect current regulation resulted in the spatial information being divided between the negative sequence carrier signal voltage and current. It should be noted that just increasing the commanded carrier current signal would

not compensate for this smearing of the spatial information due to imperfect carrier current regulation. This is due to the fact that increasing the commanded value will cause both the positive and negative sequence carrier signal currents to increase by almost the same amount with the spatial information still being divided between the negative sequence voltage and current components. It is clear that this effect can be minimized if the current regulator bandwidth is increased. Unfortunately the bandwidth of a single current regulator would have to be several times the carrier signal frequency in order to obtain the necessary regulation. This result can be seen in Fig. 7, which shows the theoretical complex vector frequency response function (FRF) [10] of a single synchronous frame PI current regulator for three different current regulator bandwidths.

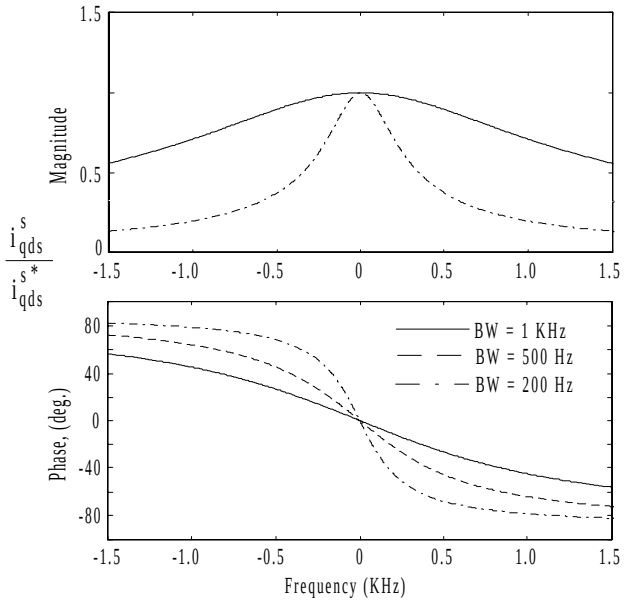

Figure 7: Theoretical Complex Vector FRF for a Single Current Regulator, Shown in the Stationary Reference Frame: Fundamental Excitation frequency = 0 Hz

Since it is possible for complex vectors to rotate in both directions, the FRF is plotted for positive and negative frequencies requiring the use of a linear frequency scale. The controller achieves the desired features of unity gain and zero phase shift only at the fundamental frequency, even if the bandwidth is 1 kHz. Another way to minimize this loss of spatial information is to decrease the frequency of the carrier signal, which is undesirable due to the reasons stated in the introduction.

IV. Current Regulator Design for Carrier Signal Rotating Vector, Current Injection

The desired ideal characteristics for a current regulator are unity gain and zero phase shift over a wide frequency spectrum. As was shown in the previous section, this is not possible with a single current regulator unless its bandwidth is almost infinite. To partially solve this problem it is possible to modify the current regulator design to get the desired properties at specifics frequencies.

To improve the regulation of the carrier signal current it is possible to modify the standard synchronous frame PI current regulator so that it properly regulates both the fundamental and carrier signal currents independent of the carrier frequency. Adding additional carrier signal synchronous frame current regulators in parallel with the fundamental component synchronous frame current regulator achieves this goal. The first possibility is to add two additional PI current regulators: one to regulate the positive sequence carrier signal component, and one to regulate the negative sequence carrier signal component, which is ideally equal to zero. Each of these additional regulators would be implemented in its respective synchronous frame, as shown in Fig. 8.

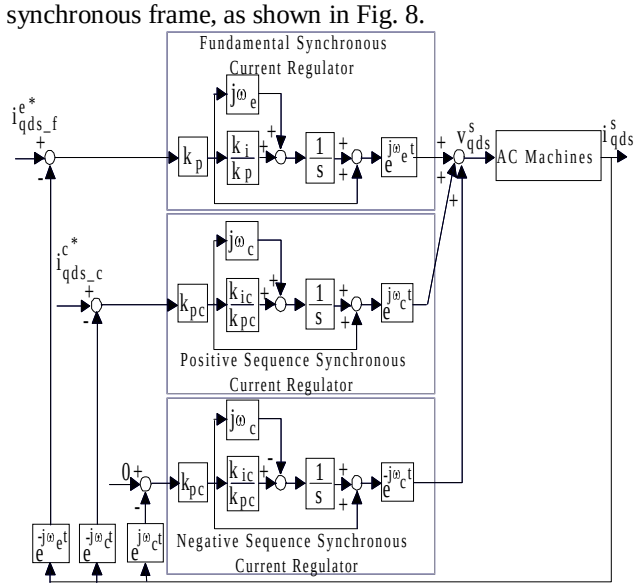

Figure 8: Block Diagram of Three Complex Vector PI Current Regulators Operating in Parallel: Each One Implemented in Its Respective Synchronous Frame

The current regulators shown in Fig. 8 are modified forms of the standard synchronous frame PI current regulator, called complex vector synchronous PI current regulators [10, 11]. The basic design theory behind this current regulator is to place the synchronous frame PI controller "complex" zero to exactly decouple the plant dynamics and cross-coupling caused by the synchronous frame transform. This cross-coupling causes the classical synchronous frame PI control system to have oscillatory dynamics, which degrade with increasing excitation frequency. By decoupling this cross-coupling, the complex vector synchronous frame PI controller achieves excitation frequency invariant dynamics.

It should be noted that when using complex vector notation, this synchronous frame cross-coupling of the machine appears as an asymmetric complex pole at $-j\omega_e$. For the case of an RL load the plant pole is located at $-R/L - j\omega_e$ in the fundamental synchronous reference frame; at $-R/L - j\omega_c$ in the positive sequence carrier signal synchronous reference frame, and at $-R/L + j\omega_c$ in the negative sequence carrier signal synchronous reference frame. For all the three current regulators the controller zeroes are designed to cancel the plant pole, including the effects caused by the synchronous frame transformation.

The remaining conventional PI gains k_p and k_{pc} are tuned to achieve the desired bandwidth of each controller. Because the carrier frequency is constant and well defined

it is not necessary to have a high bandwidth for the carrier signal current regulators.

If the carrier signal current regulators are designed to have the same bandwidth, then the only parameter that is different in both carrier controllers is the sign in the $j\omega_c$ term. Because of this, the implementation of the two carrier signal regulators can be simplified. Fig. 9 shows this simplified controller, which has the same properties as the controller shown in Fig. 8.

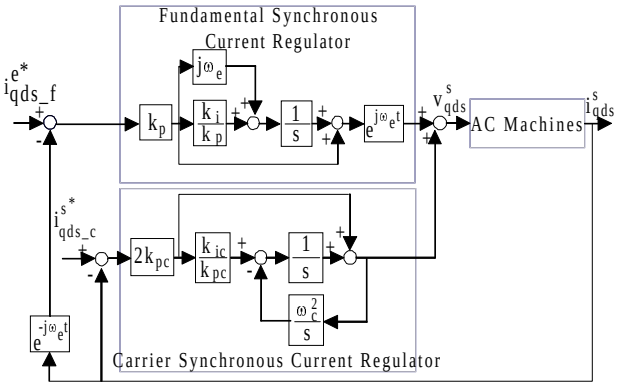

Figure 9: Block Diagram of Modified Fundamental Component Synchronous Frame - and Carrier Frequency Synchronous Frame-Current Regulators. Fundamental Regulator Implemented in Fundamental Synchronous Frame and Carrier Regulator Implemented in Stationary Frame.

The theoretical FRF of this modified current regulator is shown in Fig. 10.

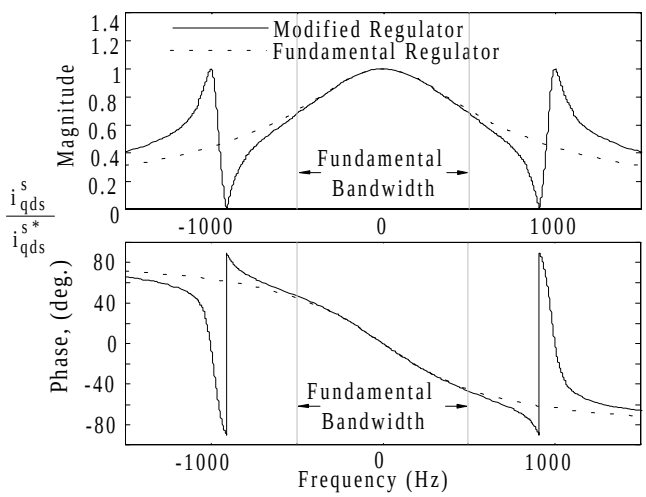

Figure 10: Theoretical Complex Vector FRF for the Modified Current Regulator, Shown in the Stationary Reference Frame: 1) Fundamental Excitation frequency = 0 Hz (500 Hz Bandwidth Regulator), 2) Carrier Frequency = 1 kHz (50 Hz Bandwidth Regulator)

The parameters of the RL load used in this figure are numerically equal to the stator transient resistance and stator transient inductance of the induction machine used in the experimental work. These parameters are shown in Table 1. It is important to note that the FRF of Fig. 10 has the desired properties of unity gain and zero phase shift at the fundamental frequency and positive and negative sequence carrier signal frequencies. This confirms that the modified current regulator is capable of regulating the fundamental excitation and both the positive and negative sequence components of the carrier signal current with no steady-state error. Furthermore, inside the fundamental current regulator bandwidth, the distortion in the FRF of the modified regulator is negligible when compared with the FRF of a single fundamental regulator. Because the carrier signal current is regulated with zero steady-state error only the impressed carrier frequency voltage (or carrier voltage command) needs to be measured for purposes of tracking the spatial saliencies.

Table 1 – Motor Parameters

Parameter	Value
R_s	0.0135 Ω
R_r	0.0140 Ω
L_{ls}	0.065 mH
L_{lr}	0.078 mH
L_m	0.530 mH
Rated speed	450 rpm
Rated torque	4.82 N-m
Rated current	120 amps
Poles	4
Stator slots	24
Rotor slots	28
Dc bus voltage	12 V

The current regulator shown in Fig. 9 was actually implemented in the discrete domain. However, even for small sampling periods, the digital regulator has degraded performance when compared to continuous-time regulator from which it was derived, especially for the case of high frequency excitation when the regulator is implemented in a stationary reference frame, as shown in Fig. 9. Because of this, care must be taken when implementing the digital form of the regulator.

Fig. 11 shows a comparison between the continuous and digital FRF's of the modified current regulator in the high frequency range.

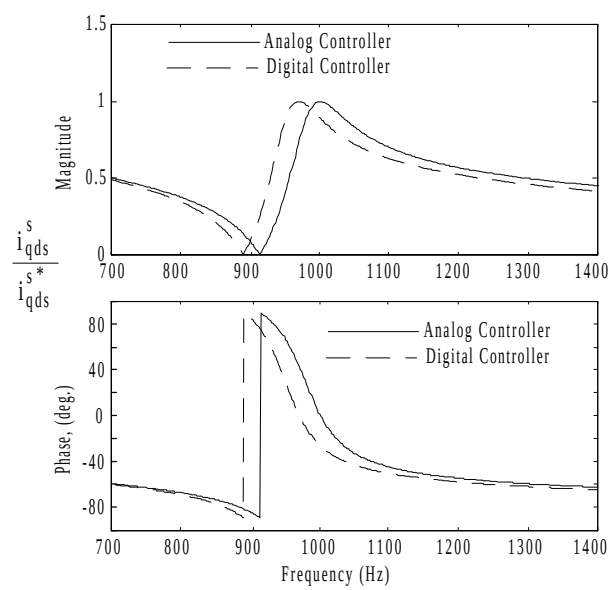

Figure 11: Comparison of the Theoretical Complex Vector FRF for the Continuous and Discrete Time Modified Current Regulator, Shown in the Stationary Reference Frame: 1) Fundamental Excitation frequency = 0 Hz (500 Hz Bandwidth Regulator), 2) Carrier Frequency = 1 kHz (50 Hz Bandwidth Regulator)

The approximation used in the digital implementation was from Tustin, (6), where T is the sampling time.

s = **Erro! Erro!** (6)

One problem with the approximation used in (6) is that the frequency scale is distorted. For instance, if it is desired to design a current regulator with the desired features of unity gain and zero phase shift at the carrier frequency ω_c, the digital current regulator obtained by the approximation (6) may not give the desired performance at the frequency ω_c. This result can be seen in Fig. 11 where the digital modified current regulator does not have the desired performance at the carrier signal frequency. Even though it is not shown, both FRF's are approximately equal in the low frequency range.

It is important in this application to design a digital regulator that closely approximates the FRF of the continuous regulator within a bandlimited range close to the carrier frequency. This can be accomplished by changing the gain of the digital controller [12]. Assume, for example, that the continuous-time carrier current regulator is designed to have the desired performance at the carrier frequency ω_c. If the digital regulator used the carrier frequency for its gain, as the continuous regulator does, distortion would result that causes the desired performance to be at a different frequency, not the carrier frequency. If the FRF of the digital current regulator is to approximate the FRF of the continuos time current regulator in the region of the carrier frequency, then the gain used in the digital current regulator, $\omega_c^{'}$, needs to be calculated as a function of the desired carrier frequency and the sample period, as shown in (6) [12].

$\omega_c^{'}$ = **Erro!** tan **Erro!** (6)

Fig. 12 shows a comparison between the FRF of the continuous and digital (with modified gain) forms of the modified current regulator in the high frequency range.

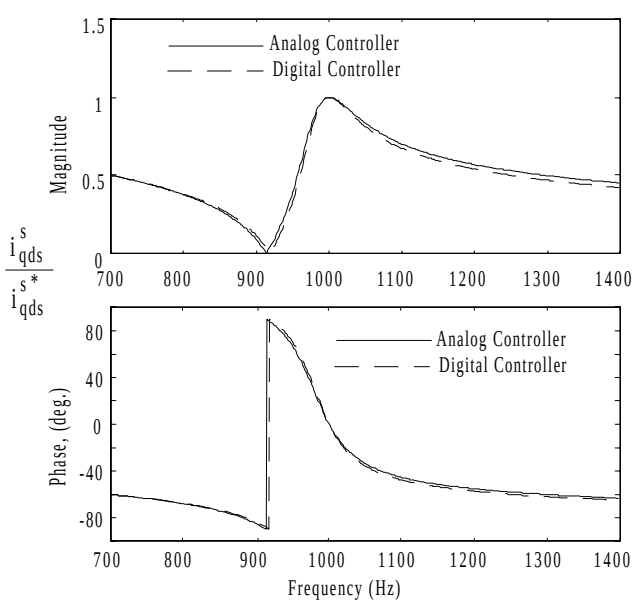

Figure 12: Comparison of the Theoretical Complex Vector FRF for the Continuous and Discrete Time (modified gains) Modified Current Regulator, Shown in the Stationary Reference Frame: 1) Fundamental Excitation frequency = 0 Hz (500 Hz Bandwidth Regulator), 2) Carrier Frequency = 1 kHz (50 Hz Bandwidth Regulator)

In this case both the continuous and discrete time regulators have approximately the same FRF in the region close to the carrier frequency, with the desired feature of unity gain and zero phase shift at the carrier frequency.

Fig. 13 shows a comparison between the actual measured voltage and current spectrums of the proposed modified controller with that of a single fundamental controller tuned for 200, 500, or 1000 Hz bandwidths (all implemented using the test machine of table 1). The figure shows only the resulting negative sequence components. The machine was running at 8.5 rpm and the carrier signal frequency was f_c = 910 Hz. In all cases the positive sequence current was adjusted to be 2.2 A, which is 2% of rated current. The theoretical value for the magnitude of the negative sequence voltage component is approximately 0.12 V.

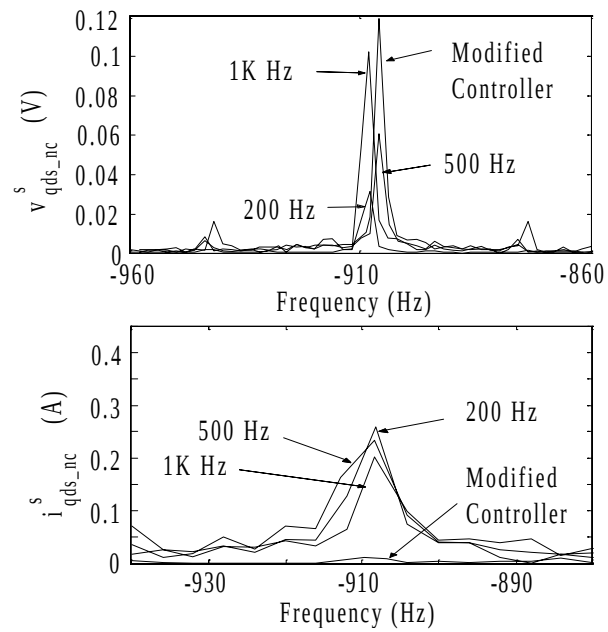

Figure 13: Measured Complex Voltage and Current Spectrums for Current Injection. Comparison of the Modified Current Regulator and Multiple Bandwidths for a Classical Synchronous Frame PI Current Regulator. (ω_r=8.5 rpm, f_c = 910 Hz)

Several conclusions can be drawn from Fig. 13. First, the modified controller is capable of regulating the carrier signal components as designed. The negative sequence carrier signal current component is approximately zero and the positive sequence carrier signal current component is equal to the commanded value

Second, the negative sequence carrier signal voltage has an amplitude equal to its theoretical value, suggesting that all of the saliency spatial information is contained in it as desired.

Third, for the case of only one controller (a classical synchronous frame PI) the saliency spatial information is divided between the negative sequence voltage and current signals. This result worsens as the bandwidth of the single controller is decreased. The single controller is unable to control the carrier signal adequately due to its limited bandwidth.

V. EXPERIMENTAL RESULTS

The extraction of the spatial information from the negative sequence carrier signal voltage is slightly different depending on whether a single current regulator or the modified current regulator is used. The signal processing steps used for both cases are shown in Fig. 14.

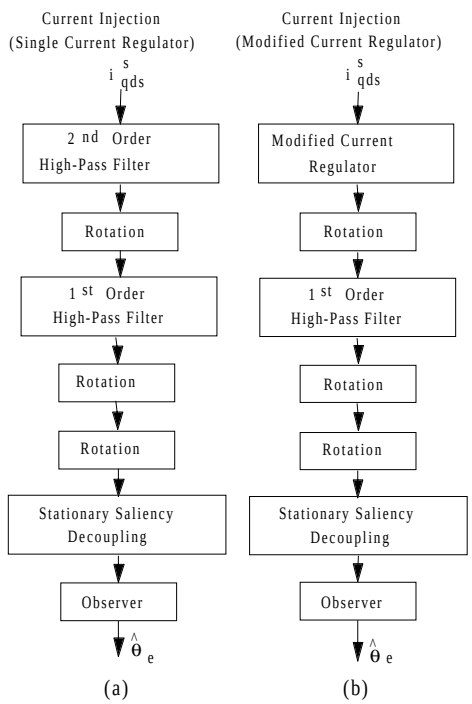

Figure 14: Signal Processing Used to Extract Spatial Information from Current Carrier Signal Injection (including Modified Design): a) Current Injection (single current regulator); b) Current Injection (modified current regulator)

The first step for the case of carrier signal current injection with a single current is to filter off the fundamental component. This is very effectively done by rotating the total stator frame signal to the fundamental synchronous frame and then applying a high-pass filter. The signal is then rotated to the positive sequence carrier synchronous frame and high-pass filtered to eliminate the positive sequence carrier signal component. The filtered signal is rotated then to the negative sequence carrier synchronous frame. In this reference frame the negative sequence carrier signal rotates with the position of the saliency, which rotates with the rotor or flux position. Furthermore, in this reference frame it is easier to decouple the effects of stationary saliencies [8]. After decoupling the stationary saliencies the tracking observer of Fig. 3 is used to estimate the saliency position. In this case the current regulator has to have a bandwidth of several times the frequency of the carrier current signal to ensure that there is no distortion or smearing of the spatial information. Although possible, this high of bandwidth is not practical for the frequency of the carrier signals used in this paper.

For the case of carrier signal current injection with the modified current regulator, the differences in the signal processing are the inclusion of the modified current regulator and the elimination of the high-pass filter used to filter off the fundamental excitation. Filtering of the fundamental excitation is not necessary since the signal used in this case is the voltage command from the output of the carrier synchronous current regulator (see Fig. 8). The filtering properties of this regulator achieve the goal of eliminating the fundamental component.

Table 2 shows the processing requirements for each technique. As can be seen, the total number of adds and multiplies is the same for both cases.

Table 2 – Processing Requirements

	Current Injection	
	Single "i" Regulator	Modified "i" Regulators
Rotations	4	3
adds	8	6
multiplies	16	12
Filters	2	1
adds	8	4
multiplies	8	4
Regulators	0	1
adds	0	8
multiplies	0	8
Observer	1	1
adds	4	4
multiplies	5	5
Total		
adds	20	22
multiplies	29	29

With carrier signal current injection the current regulator directly limits the bandwidth of the estimate. Fig. 15 shows the experimentally measured estimation accuracy FRF ($\hat{\theta}_r/\theta_r$) for carrier signal current injection.

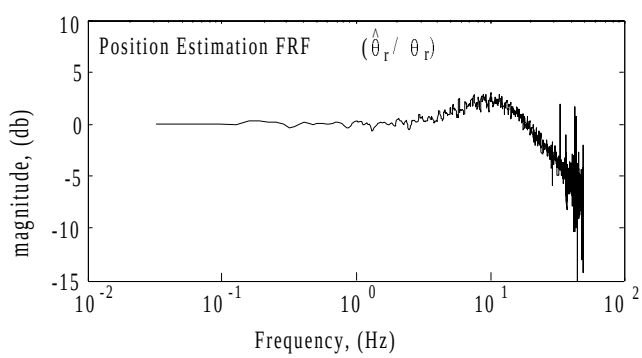

Figure 15: Measured Frequency Response of the Rotor Position Estimation Using Current Carrier Signal Injection

The observer and the carrier synchronous current regulator bandwidth were both tuned for approximately a 50 Hz bandwidth. The difference between the tuned observer bandwidth and the experimental estimation bandwidth is due to the fact that the observer bandwidth is affected by both the carrier signal voltage level and the current regulator bandwidth [8]. For this example the measured estimation bandwidth is approximately 33 Hz. The filtering provided by the current regulator does produces a "clean" signal (less ripple on the estimate). Obviously if the carrier synchronous current regulator was tuned to give a bandwidth higher than the observer bandwidth the estimation bandwidth would be limited by the observer. Unfortunately, the bandwidth of the carrier synchronous current regulator must be limited to prevent it from

distorting the bandwidth of the fundamental current regulator.

The experimental results shown for the estimation FRF are not the highest that was achievable with the current regulator bandwidth used for the experimental results. Instead the observer bandwidth was deliberately detuned to make the FRF measurement easier. It is possible to tune the observer to give higher estimation bandwidths, but it becomes more difficult to accurately measure the FRF. The FRF shown in Fig. 15 was measured using a spectrum analyzer and a random noise excitation with a constant power frequency spectrum. At high frequencies the signal power was not high enough to cause large movements in the rotor position. This results in the degradation of the experimental FRF as the frequency increases.

Using an induction machine with a deterministic ±10% (of rotor leakage) rotor slotting saliency (see Table 1), rotor position estimation was implemented using carrier signal current injection with the modified current regulator. Fig. 16 shows an overlay of the experimentally estimated and measured rotor position and error obtained using the modified current injection system for a speed command from 0 rpm to -15 rpm to 15 rpm, and back to 0 rpm. A carrier frequency of 1 kHz was used for this test, significantly higher than used in previously published results using carrier signal current injection. As can be seen from the figure, the estimated rotor position follows the actual rotor position quite well, even at zero speed.

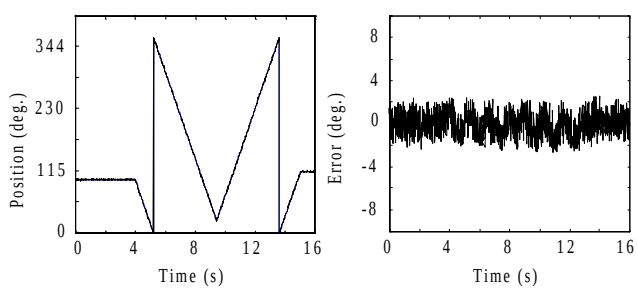

Figure 16: Overlay of Experimentally Estimated and Measured Rotor Position, and Error for Steps in the Rotor Speed (0 rpm to -15 rpm to 15 rpm to 0 rpm) Using Current Injection via the Modified Regulator

VI. Conclusions

Injection of a carrier signal current into a salient machine produces impressed voltages that contain information relating to the spatial position and magnitude of the saliency.

A tracking observer can be used to extract the spatial position information and provide wide bandwidth estimates of the flux, rotor position, and velocity, at virtually all speeds and frequencies, including low and zero speed/frequency.

The carrier signal frequency selection for current injection should be high enough so that an impedance-based voltage gain is realized and the estimation bandwidth is not severely limited. Since the rotor flux linkage deteriorates with higher frequencies there is a diminishing return to very high frequencies. Thus, the carrier frequency can be optimized.

The simplest measurement approach for current injection would regulate the carrier frequency current amplitude such that only the impressed carrier frequency voltage signal (voltage command) would be necessary for flux, position, and velocity estimation. This is analogous to voltage injection whereby the carrier voltage amplitude is regulated such that only the resulting carrier current needs to be measured.

The key to injecting a small amplitude carrier signal current at a relatively high frequency is having a current regulator capable of regulating both the fundamental and carrier signal current commands with almost no error. The use of properly designed, parallel-operating current regulators was shown to resolve this problem.

Acknowledgments

The authors wish to acknowledge the financial support and motivation provided by the Ford Motor Company, CNPq-Brazil, and the Wisconsin Electric Machines and Power Electronics Consortium (WEMPEC) of the University of Wisconsin – Madison.

References

[1] Jansen, P.L., Lorenz, R.D., "Transducerless Position and Velocity Estimation in Induction and Salient AC Machines", *IEEE Trans. on Industry Applications*, Mar/Apr 1995, pp. 240-247.

[2] Jansen, P.L., Lorenz, R.D., "Transducerless Field Orientation Concepts Employing Saturation-Induced Saliencies in Induction Machines", *IEEE Trans. on Industry Applications*, Vol. 32, No. 6, November/December 1996, pp. 1380-1393.

[4] Corley, M.W. and R.D. Lorenz, "Rotor Position and Velocity Estimation for a Permanent Magnet Synchronous Machine at Standstill and High Speeds", *Proc. IEEE-IAS Annual Meeting*, San Diego, CA, October 1996, pp. 36-41.

[5] Blaschke, F., Burgt, J, and Vandenput, "Sensorless Direct Field Orientation at Zero Flux Frequency", in *IEEE, IAS Conf. Rec.*, Oct 5-10, 1996, pp. 189-196.

[6] Ha, J., and Sul, S., "Sensorless Field Orientation Control of an Induction Machine by High Frequency Signal Injection", *Proc. IEEE-IAS Annual Meeting*, New Orleans, October 1997, pp. 426-432.

[7] Degner, M.W., Lorenz, R.D., "Position Estimation in Induction Machines Utilizing Rotor Bar Slot Harmonics and Carrier Frequency Signal Injection, M.W. Degner, R.D. Lorenz, *Proc. PCC Nagaoka Technical Conference*, Nagaoka, Japan, August, 1997, pp. 69-72.

[8] Degner, M.W., Lorenz, R.D., "Using Multiple Saliencies of the Estimation of Flux, Position, and Velocity in AC Machines", *IEEE-IAS Annual Meeting*, New Orleans, LO, October 1997, pp. 760-767.

[9] Cilia, J., Asher G.M., Bradley, K.G., "Sensorless Position Detection for Vector Controlled Induction Motor Drives Using an Asymmetric Outer-Section Cage", *Proc. IEEE-IAS Annual Meeting*, San Diego, CA, October 1996, pp. 286-292.

[10] Briz, F., Degner, M.W., and Lorenz, R.D., "Analysis and Design of Current Regulators Using Complex Vectors", *Proc. IEEE-IAS Annual Meeting*, New Orleans, October 1997.

[11] Briz, F., Degner, M.W., and Lorenz, R.D., "Dynamic Analysis of Current Regulators for AC Motors Using Complex Vectors ", *Proc. IEEE-IAS Annual Meeting*, St. Louis, October 1998.

[12] Aström, K.J, and Wittenmark, B. "Computer Controlled systems: Theory and Design", Prentice Hall, 3rd ed., 1997.